

EFFECT OF EXTERNAL STORES AERODYNAMICS ON ANALYTIC FIGHTER AIRCRAFT FLUTTER PREDICTIONS: EVALUATION OF A SUPERPOSITION MODELING APPROACH

Maj. Michael Iovnovich¹

¹Flight Sciences Branch
Israeli Air Force
Tel-Aviv, Israel
smichael.iov@gmail.com

Keywords: Flutter analysis, Unsteady Aerodynamics, Reduced Order Modeling, Computational Aeroelasticity

Abstract: Flutter instability prediction of fighter aircrafts capable of carrying an extensive external stores inventory typically requires analytic assessment of thousands of configurations throughout the operational flight envelope. To enable realistic solution times, simplified unsteady aerodynamics models are commonly used, in which underwing stores aerodynamics is neglected. In the current study, the effects of underwing stores aerodynamics on flutter prediction capabilities are assessed using a heavyweight store configuration of the F-16 aircraft with multiple underwing stores and in correlation with flight test data. This examination is conducted at the high transonic flow regime using two unsteady aerodynamics solvers, namely, the linear, panel-based ZAERO solver and the nonlinear, Euler, ZEUS solver. This investigation showed that underwing stores modeling may in-fact considerably affect the predicted flutter onset speeds. Neglecting stores aerodynamics yielded both less realistic and nonconservative predictions by both ZAERO and ZEUS models. The comparison between the ZAERO and ZEUS models solutions revealed significant differences in steady and unsteady surface pressure distributions due to nonlinear flow phenomena. These differences also manifested in significant distinctions between the two models flutter predictions. To enable full aerodynamic modeling in industrial flutter survey applications, a superposition modeling approach is formulated and successfully validated using the studied test case. According to this method, introduction of a new store into the aircraft weapons inventory will only require a single aerodynamic model solution, then aerodynamic models for configurations including any permutation of the new store with other pre-existing stores in the database may be directly assembled with no additional computations required. This technique is found effective for superposition between linearized unsteady aerodynamics stores effects, even if the base flow of these effects is nonlinear. However, once interference between stores becomes dominant and nonlinear, this modeling approach is no longer valid.

1 INTRODUCTION

Aeroelastic instability certification of an aircraft deals with the dynamic characteristics of the aircraft inertial, elastic and aerodynamic models coupling. Any significant variation in these models may affect the stability conditions and therefore shall be addressed in the certification process. Typical variations include inertial changes due to fuel consumption, aerodynamic variations due to flight conditions and both elastic and aerodynamic model variations due to external

stores installation. A fighter aircraft, capable of carrying an extensive weapons and stores inventory on multiple structural stations, significantly increases the complexity of the process. In general, an aircraft with I representative internal inertial states and S store stations capable of carrying M different stores on each station will require at least $I \cdot S^M$ aeroelastic unique configurations to be analyzed. For typical fighters, this may sum up to thousands of cases.

A Typical certification process may be divided into analytic investigation, in which all relevant configurations are analyzed and critical cases are identified, and ground/flight test investigations, in which only a small number of configurations are tested to validate the analytic models or to obtain a reliable clearance of the aircraft operational envelope. Analytic investigations typically rely on structural dynamics and unsteady aerodynamics models which are coupled in a stability flutter analysis. The dynamic model consists of finite-element mass and stiffness representations of the structure and used to identify the structural natural frequencies and mode shapes by means of a modal analysis eigenproblem. The unsteady aerodynamic model consists of discrete external geometry representation which is used to solve flow equations in order to obtain the aerodynamic responses to structural excitations. The flutter analysis is commonly formulated as a complex, nonlinear, eigenproblem of the frequency-domain aeroelastic equations of motion which is solved in generalized (modal) coordinates, therefore all structural and aerodynamic terms are eventually obtained in modal coordinates. Dynamic models which are adequate for flutter analyses may include up to a few hundreds of degrees of freedom (DOFs), while more complicated models may be reduced with little effect on the results by means of model condensation methods such as the guran reduction method [1]. With modern computational resources available, modal analysis of such models is unchallenging, even for thousands of configurations. Furthermore, these models may be easily decomposed into structural components and then reconstructed in an automated configuration assembly process. On the other hand, detailed aerodynamic models typically include between one to four orders of magnitude more DOFs compared to dynamic models, depending on the aerodynamic solver used. Reduction of an aerodynamic model usually directly affects its fidelity and therefore shall be avoided. Furthermore, the aerodynamic solution process is more computationally demanding compared with a modal analysis solution and is repeated for several Mach numbers and reduced frequencies for each of the analyzed aerodynamic configurations. This makes full aerodynamic modeling for each analyzed aeroelastic configuration currently impractical.

Aerodynamic modeling for aeroelastic analysis purposes may be divided into traditional linear panel methods and high-fidelity computational fluid dynamics (CFD) methods. Panel methods are used to solve the inviscid, compressible, unsteady, linearized small-disturbance potential equation for subsonic and supersonic flows to obtain an unsteady pressure coefficient solution on each surface panel of the configuration due to harmonic deflection perturbation in each of the other panels. This solution is then integrated into the aerodynamic influence (force) coefficient (AIC) matrix and transformed into structural coordinates at the dynamic model DOFs by means of a spline transformation [2]. From the structural DOFs, the aerodynamic forces are transformed into generalized (modal) coordinates using the structural mode shapes to obtain the generalized aerodynamic force (GAF) matrix which is then used in the flutter solution. Since the AIC matrix itself is invariant of the structural mode shapes, it may be used for multiple aircraft configurations of similar geometry and variable dynamic properties. This feature simplifies aerodynamic modeling for multiple configuration analyses, nevertheless, the vast amount of external store permutations of a fighter aircraft still requires recalculation of the AIC matrix for each geometrically unique case. Panel methods are considered the industrial standard in the aeroelasticity community and are implemented in the popular NASTRAN [3] and

ZAERO [4] software; even so, its deficiency comes in the high transonic flow regime, where the appearances of supersonic bubbles and shock waves along non-flat lifting surfaces, which are neglected by the linear theory, may result in nonlinear flutter behavior such as the transonic dip phenomenon [5]. CFD methods for aeroelastic predictions are used to solve various versions of the nonlinear Navier-Stokes flow equations and thereby offer improved modeling capabilities in the presence of flow nonlinearities [6,7]. The most popular application of such methods to flutter prediction is focused on obtaining unsteady aerodynamics reduced order models (ROMs) using direct calculation of GAF matrices by linearization of the aerodynamic responses in the time-domain to broadband structural excitation of each of the analyzed configuration mode shapes and identification of the aerodynamic transfer functions in the frequency-domain by means of Fourier transforms. Although CFD methods were shown to offer reliable correlations with test data of challenging cases [8], their increased computational effort currently limits industrial applicability to cases of special interest.

The problem of aerodynamic modeling of multiple external store configurations is often resolved by considering a simplified aerodynamic model which is assumed to represent a large set of aeroelastic configurations. Since both the AIC and spline models are invariant of the structural dynamic properties, these simplified models may be obtained and transformed into structural coordinates once and then applied to various configurations of different dynamic properties with no additional computational cost. For fighter aircrafts, such simplified models usually include a clean wing with wingtip stores, as wingtip aerodynamics is shown to play a key role in the flutter solution. According to such methodology, the aerodynamic contributions of the rest of the stores in the configuration are neglected. This approach is argued to be both conservative and practical, suggesting that store aerodynamics at inboard wingspan stations tend to increase the overall aerodynamic damping of the flutter-relevant modes and may generally be covered by the analysis safety margins. This argument is only partially supported by previous investigations available in the literature. Turner [9] conducted parametric investigation of various underwing and wingtip stores/missiles on four fighter aircraft wing platforms. The investigation was conducted using the NASTRAN aerodynamic doublet lattice method (DLM) [10] solver. Results indicated that only 60% of test configurations resulted in flutter speed variations lower than 7% due to store aerodynamics, while for the rest of the cases higher variations were obtained. Later studies [11–13] used the ZAERO implementation of the ZONA6 [14] panel method. These studies examined several store configurations of the F-16 aircraft with various stores. Comparison between different aerodynamic models showed up to 17% of variation in flutter velocities due to underwing stores aerodynamics. Terashima [15] used a CFD aeroelastic model of a delta wing with an underwing store to show that shock waves, which are generated ahead of the store in supersonic flow, may affect the wing lower surface pressure distribution and lead to considerable decrease in the flutter speeds.

To reduce the aerodynamic modeling effort for configurations with external stores, Chen et al. [11] suggested a superposition methodology for the AIC matrix calculation. According to this method, store-to-store and aircraft-to-store influence submatrices are stored in a database and assembled into a full AIC for each external store configuration. Since this approach is formulated in the aerodynamic DOFs, it requires direct access to the aerodynamic solution application, namely the ZAERO software, which limits its applicability to other flutter solution tools. Karpel et al. [16] suggested another superposition approach for GAF matrices assembly. According to this approach, incremental store GAFs may be derived as a subtract between wing+store GAF and a clean wing GAF, then the full GAF may be assembled for each store configuration based on the incremental GAFs. This approach requires the use of the fictitious

mass approach [17] for modal coupling between the main structure and the underwing stores. This approach is limited in modeling structurally complex stores and pylon interfaces.

The current study evaluates the effects of underwing stores aerodynamics on the flutter solution using a heavy store configuration of the F-16 fighter aircraft with various underwing stores. This examination is conducted at the high transonic flow regime using two modeling tools, namely the ZAERO [4] panel solver and the ZEUS [18] Euler solver. Once store aerodynamics significance is demonstrated, a computationally efficient store aerodynamic modeling superposition approach is formulated in structural coordinates and validated using the studied test case.

2 THEORETICAL MODEL

For the current derivation, N_a is identified as the number of aerodynamic model DOFs, namely surface panels for panel method models and surface mesh panels or centroids for CFD based solvers. N_s is identified as the number of structural DOFs in the finite element model and N_m is identified as the number of structural mode shapes to be included in the analysis. The mode shapes matrix $\Phi \in \mathbb{R}^{N_s \times N_m}$ is available from modal analysis of the dynamic model and the spline matrix $G \in \mathbb{R}^{N_a \times N_s}$ is obtained as the spline transformation from the structural model to the aerodynamic model. The spline matrix is assumed to be invariant of the structural dynamic properties according to [2].

A panel method solution yields the following aerodynamic models in aerodynamic (AIC), structural (AFC) and modal (GAF) DOFs:

$$AIC(ik) \in \mathbb{C}^{N_a \times N_a} \quad (1)$$

$$AFC(ik) = G^T \cdot AIC \cdot G \in \mathbb{C}^{N_s \times N_s} \quad (2)$$

$$GAF(ik) = \Phi^T \cdot AFC \cdot \Phi \in \mathbb{C}^{N_m \times N_m} \quad (3)$$

where k is the aerodynamic reduced frequency. Elements $AIC_{i,j}$, $AFC_{i,j}$ and $GAF_{i,j}$ represent the unsteady aerodynamic force response in DOF i due to deflections of DOF j . Alternatively, a CFD ROM solution directly yields the $AFM(ik) \in \mathbb{C}^{N_a \times N_m}$ matrix in which element $AFM_{i,j}$ represents the response in aerodynamic DOF i due to harmonic modal excitation in mode j . Consequently, the GAF matrix can be directly calculated by:

$$GAF(ik) = \Phi^T \cdot G^T \cdot AFM \in \mathbb{C}^{N_m \times N_m} \quad (4)$$

This model can not be injectively transformed into structural coordinates, however the AFC model may be estimated in the least square sense by pseudo-inverse of the modes matrix according to:

$$AFC(ik) = G^T \cdot AFM \cdot \Phi^+ \in \mathbb{C}^{N_s \times N_s} \quad (5)$$

2.1 Superposition of AFC matrices

The suggested approach focuses on decomposition of the AFC matrix into basic submatrices which represent specific structural components. Such submatrices may be extracted from relatively simple aerodynamic models in which only the relevant structural components are included, then more complicated aerodynamic models may be constructed by assembly of multiple component submatrices. Looking at a fighter aircraft with multiple external wing store

stations, DOF_i is identified as the structural DOFs set which represent store station i . The AFC_i submatrix is identified as:

$$AFC_i(ik) = AFC_{DOF_i, DOF_i} \in \mathbb{C}^{DOF_i \times DOF_i} \quad (6)$$

This extraction neglects mutual effects between DOF_i and the rest of the structural DOFs, therefore interference between the store station and the wing, as well as interference between adjacent store stations are excluded. To minimize the effect of this assumption, wing structural DOFs near the store station may be included in the submatrix extraction. By repeating this process for all store stations, a store aerodynamic force influence database may be built. Such database may be built by solving a clean aircraft model with each of the possible stores at each possible carrying station. A full aircraft configuration AFC matrix can then be constructed by assembly of a clean aircraft AFC submatrix with the relevant stores submatrices. If wing-to-station interference effects are accounted in the submatrix extraction process, the overlapping wing DOFs shall be compensated by subtraction of the relevant DOFs AFC elements using the clean aircraft model. This superposition process is illustrated geometrically in Figure 1 for a single store configuration. In this illustration, the red box identifies the parts of the model which are assembled in each stage of the process, namely the DOF_i bounds. According to this method, introduction of a new store into the aircraft weapons inventory will only require a single aerodynamic model solution, then aerodynamic models for configurations including any permutation of the new store with other pre-existing stores in the database may be directly assembled with no additional computations required.

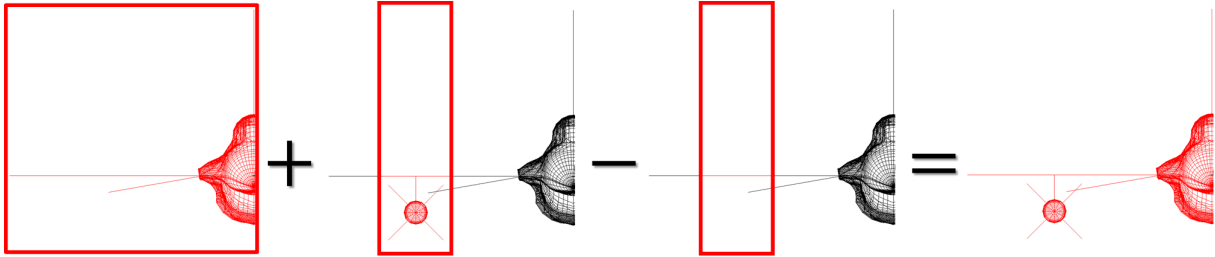


Figure 1: Aerodynamic model superposition process illustrated

The benefits of the suggested approach over previous formulations are listed below:

- It is applicable to any unsteady aerodynamics solution method or software, including panel solvers and CFD-based solvers, as demonstrated in the current study
- Its application does not require direct access to the solver code
- It is applicable to structurally unique stores and does not rely on modal coupling techniques
- AFC databases typically require small storage space and short assembly times
- AFC superposition is preferable over GAF superposition for structural dynamic response applications such as gust, landing and store ejection response loads since loads calculations are typically conducted in structural DOFs

3 TEST CONFIGURATION

A heavyweight, full-span, symmetric configuration of the F-16 aircraft is used in the current study as a test case. Description of the stores within the configuration is presented in Table 1. This configuration was investigated in flutter flight tests (FT) in which anti-symmetric limit cycle oscillations (LCO) were monitored at several flight conditions. At Mach 0.95, mild LCO

was monitored at some specific dynamic pressure conditions along with very low damping levels that were identified prior to that LCO occurrence. Since LCO typically occurs near the flutter boundary and based on the low damping indication, LCO onset conditions are evaluated from the flight test data and used as a reference boundary for the analytic flutter predictions presented in this study at Mach 0.95.

Store station	Span location	Store
1/9	Wingtip	Missile launcher
2/8	Outboard	Air-to-Air missile
3/7	Midspan	Air-to-Ground Store
4/6	Inboard	600 Gallon fuel tank
5	Centerline	300 Gallon fuel tank

Table 1: Description of the F-16 test store configuration

3.1 Dynamic Model

The F-16 dynamic model is a general element type of model that was constructed and validated through ground vibration tests by the aircraft manufacturer. The model is presented in Figure 2. The test configuration model includes about 500 structural DOFs. For this configuration, all stores are modeled as point masses that are attached to the various store stations, although the suggested aerodynamic model superposition methodology is applicable to any type of structural store station model.

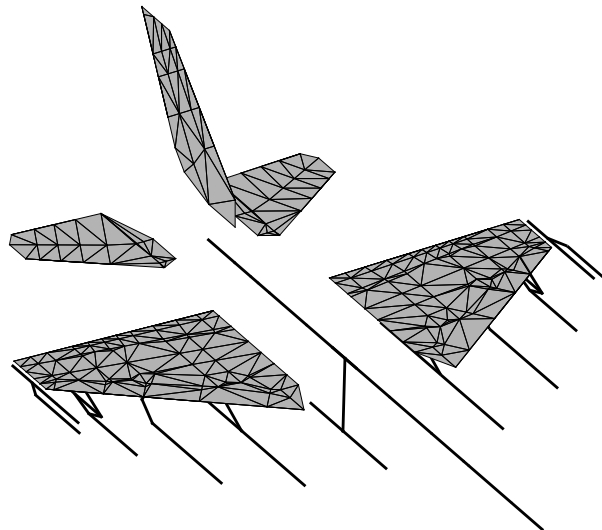


Figure 2: Dynamic model of the F-16 aircraft

3.2 Aerodynamic Models

Two solvers are used in the current study, namely ZAERO [4] and ZEUS [18]. ZAERO is a linear, panel based, solver which is the industrial standard for flutter predictions. ZEUS is an overset, Cartesian grids, nonlinear Euler solver which is built on the aeroelastic foundations of ZAERO, and thereby supports valuable capabilities for straightforward unsteady aerodynamics modeling for aeroelastic applications. These capabilities include the mesh auto-generator, 3D spline modules and a variety of unsteady aerodynamic ROMs generation modules. In the current study, frequency domain ROMs are generated in ZEUS using the linearized euler solver [19],

in which each column of the AFM matrix is obtained by a steady-state solution of the flow perturbation equations, while the nonlinear steady flow field is only solved once in the ROM generation process. For the ZAERO analyses, the ZONA6 subsonic solver was used.

Both ZAERO and ZEUS use a panel geometry discretization model on which the unsteady aerodynamic solution is obtained. Figure 3 presents the panel models for both solvers, which are geometrically similar except for some minor adjustments. The ZAERO model consists of about 12,000 panels, while the ZEUS surface model consists of about 20,000 panels, mainly due to finer fuselage surface discretization. Figure 4 presents the ZEUS model Cartesian grid blocks for the vertical tail and stores. The global grid block accommodates the main aircraft geometry as well as the wintip launchers. The second-level overset hierarchy grid blocks are the underwing and centerline stores body grids, which are presented for the right wing stores on Figure 5. The third-level hierarchy grid blocks are the pylons and stores fins and canards blocks, which are presented for the left wing stores on Figure 5. Overall, the full configuration ZEUS model includes about 3.5M grid cells. To obtain the unsteady aerodynamic solution in ZEUS, the steady flow solution was iterated for 150 steps at 3° angle of attack and $CFL=7.0$. The flow perturbation solution was obtained for each reduced frequency and mode shape per by an 80 iterations solution at $CFL=6.0$. This numerical setup was sufficient to achieve residual convergence of at least 3 orders of magnitude for all blocks.

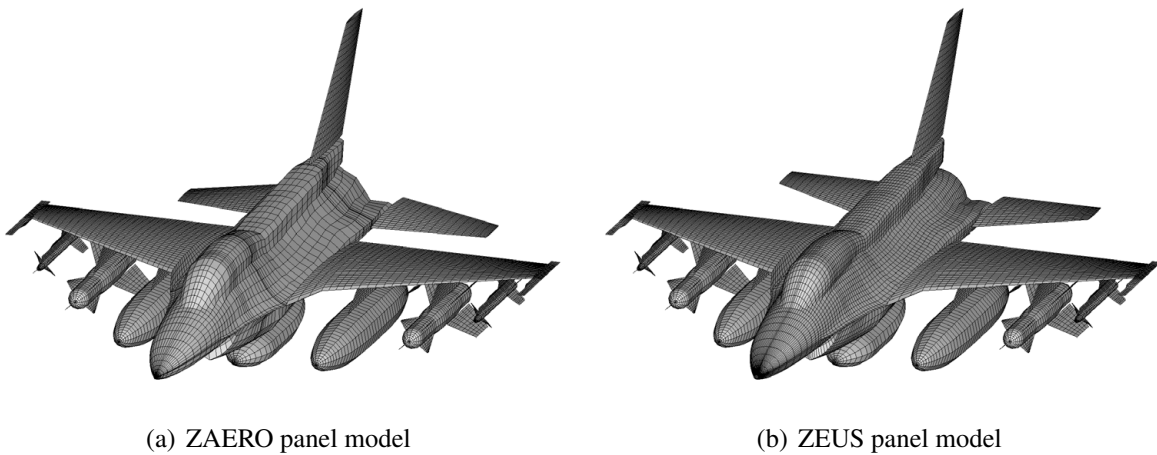


Figure 3: ZAERO and ZEUS panel models of the test configuration

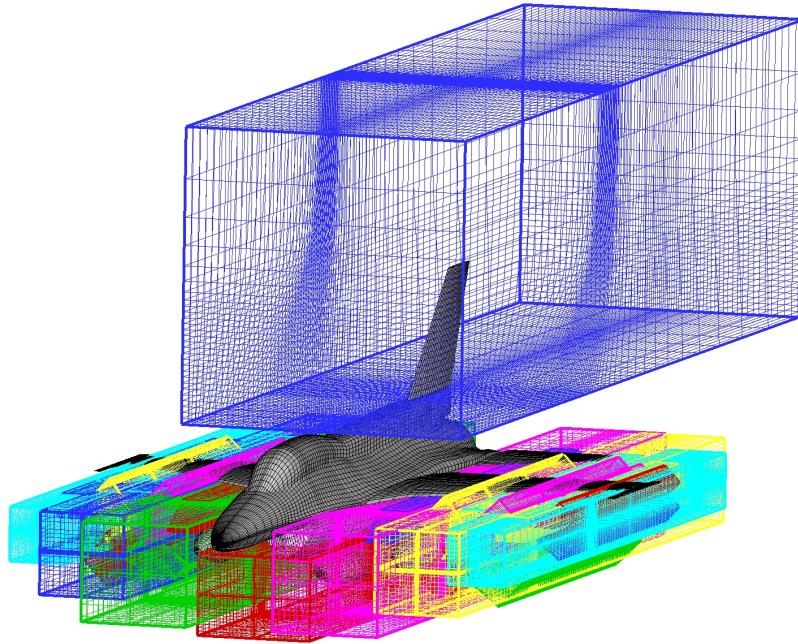


Figure 4: ZEUS model overset grids

For spline transformation between the dynamic and aerodynamic models, infinite plane type of spline was used for the aircraft lifting surfaces and store pylons/launchers, a beam type of spline was used for the aircraft fuselage and a rigid-body motion type of spline was used for all external stores including their lifting surfaces.

AFC matrices were obtained from ZAERO and ZEUS as detailed in the Theoretical Model section. To apply the AFC superposition methodology, component AFC_i submatrices were extracted for each store based on solutions of a clean aircraft with a single store models. The DOF_i set bounds, which are represented by the red boxes in Figure 1, are adjusted to each store station to obtain adequate correlation between the reconstructed and full AFC models, as demonstrated in the results section.

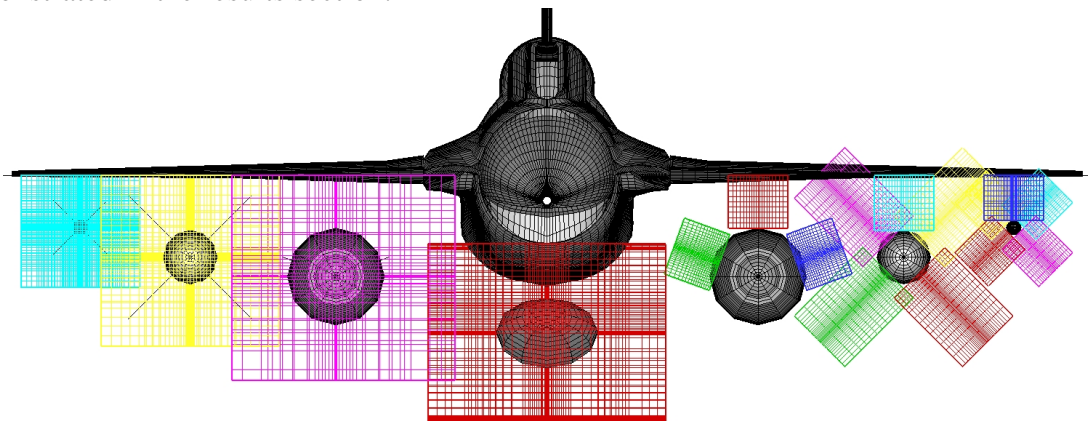


Figure 5: ZEUS model overset grids

3.3 Mode Shapes

Figure 6 presents the four flutter-relevant natural mode shapes of the test configuration, mapped on the full aerodynamic ZAERO model. In order to isolate aerodynamic modeling effects, the dynamic properties are kept constant throughout the investigations presented in the current study, i.e. the same set of modes is used for all aerodynamic configurations, regardless of which stores are taken into account aerodynamically.

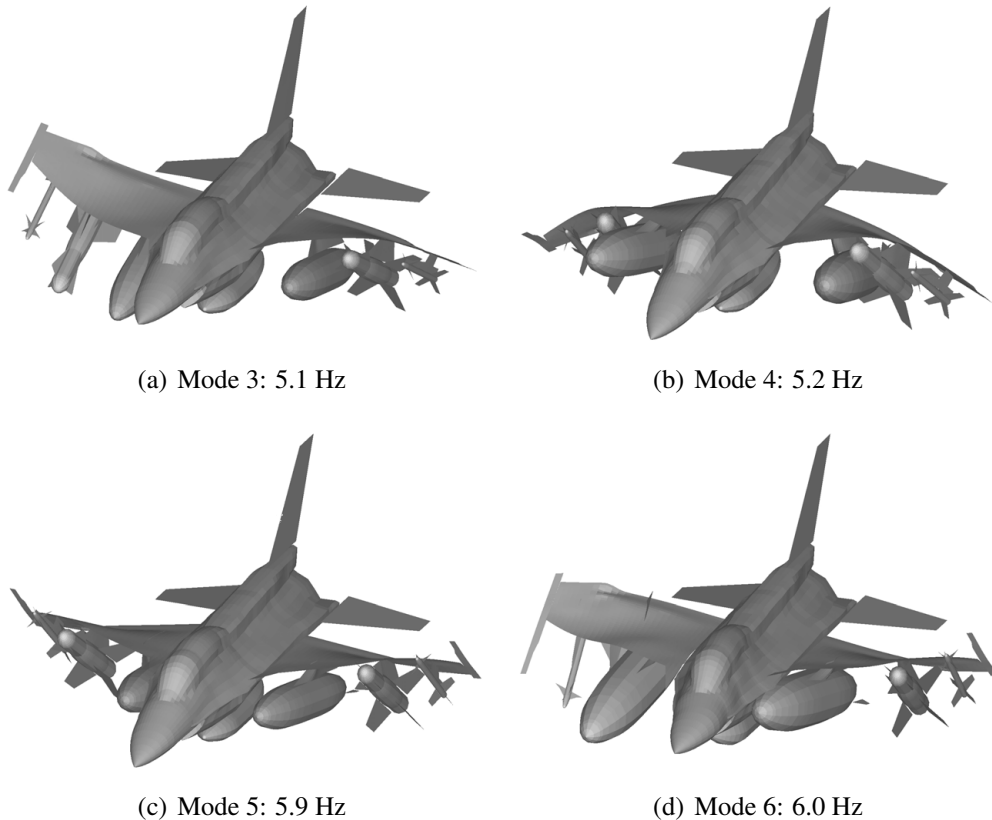


Figure 6: Four natural mode shapes mapped on the aerodynamic panel model

3.4 Flutter Mechanisms

In this study, flutter solutions are conducted using an IAF in-house automated configuration assembly and flutter solution tool. The matched-point G-method damping perturbation solver implementation by Gu and Yang [20] with first order damping term is used. Figure 7 presents frequency/damping vs. normalized equivalent airspeed (EAS) curves for the flutter coupling modes of the test configuration at Mach 0.95 based on the ZAERO and ZEUS aerodynamic models. These results are obtained using a basic aerodynamic model in which only the wintip launchers are included. For both models, two flutter mechanisms are identified: a symmetric (SYM) mechanism involving modes 4 and 5 and an anti-symmetric (A/S) mechanism involving modes 3 and 6. FT LCO onset conditions are marked by a red dashed line. The FT LCO mode was of A/S motion, therefore its onset conditions are relevant for the A/S mechanism. As structural modal damping coefficients of the test configuration are unknown, $G_s = 2\%$ was assumed in the solution for all modes. Since physical structural modal damping coefficients may vary in the range of $G_s = [0.5 - 2.5]\%$, flutter onset conditions may be evaluated as modal damping crossings in the damping margins range of $G = [-1.5 - 0.5]\%$. These damping margins are indicated in the damping plots.

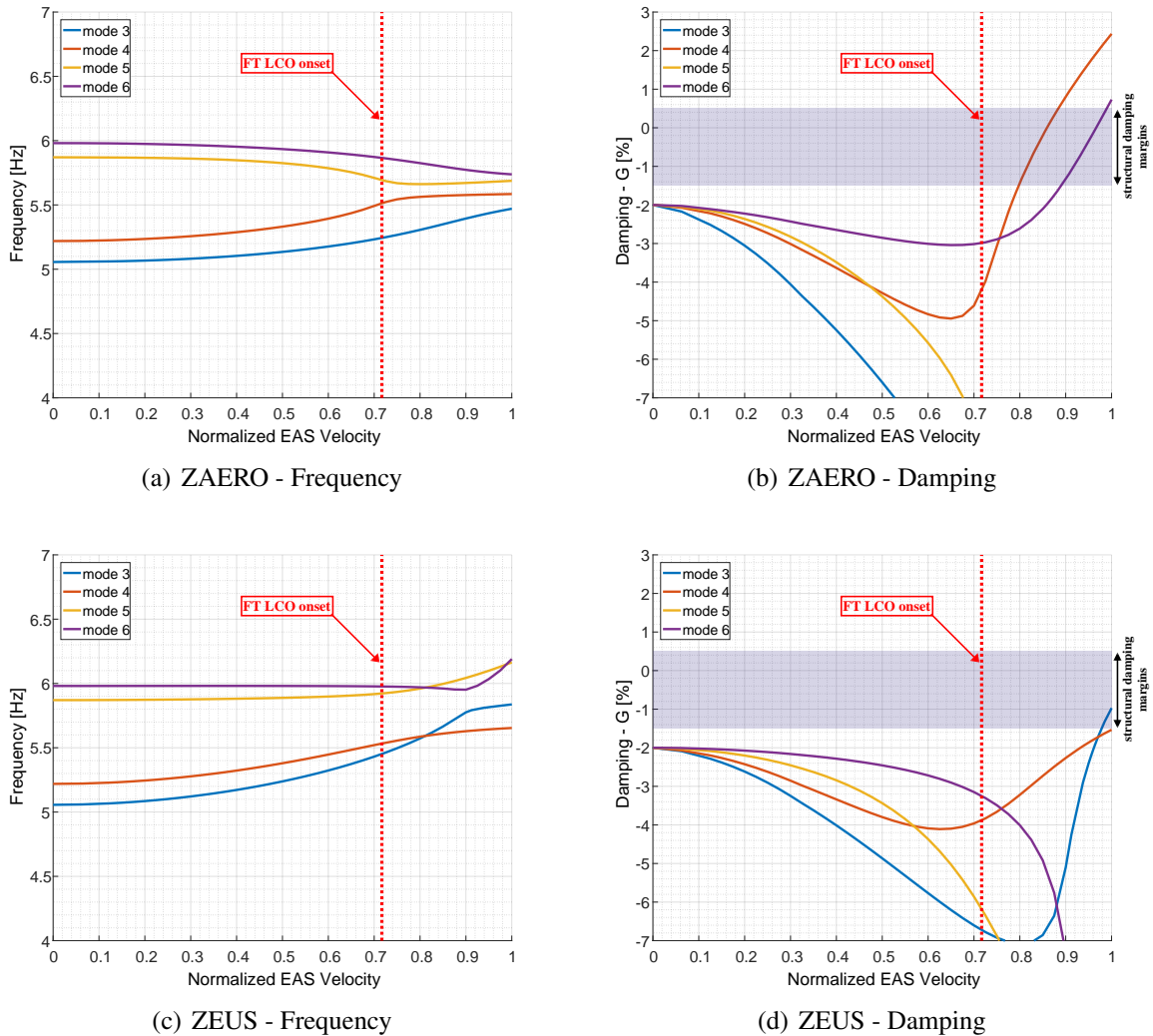


Figure 7: Flutter analysis results using basic aerodynamic models, Mach 0.95

Comparing between the ZAERO and ZEUS aerodynamic models predictions, two main differences are identified: both mechanisms are predicted at 10-20% higher EAS and frequency shifts are more apparent in the ZEUS prediction compared with ZAERO. The ZAERO model predicts lower flutter speeds for the SYM mechanism than for the A/S mechanism, which contradicts the FT A/S LCO indication. In the ZEUS model prediction, the SYM mechanism is a hump mechanism. Compared to the FT A/S LCO boundary, the A/S mechanism flutter onset speeds are overpredicted by about 20% and 30% by the ZAERO and ZEUS models, respectively. Figure 8 presents a single snapshot of both mechanisms complex flutter modes. It is indicated that the SYM mechanism mainly involves wing bending, while the A/S mechanism mainly involves wing torsion. These basic mechanism characteristics are similar between the ZAERO and ZEUS models analyses.

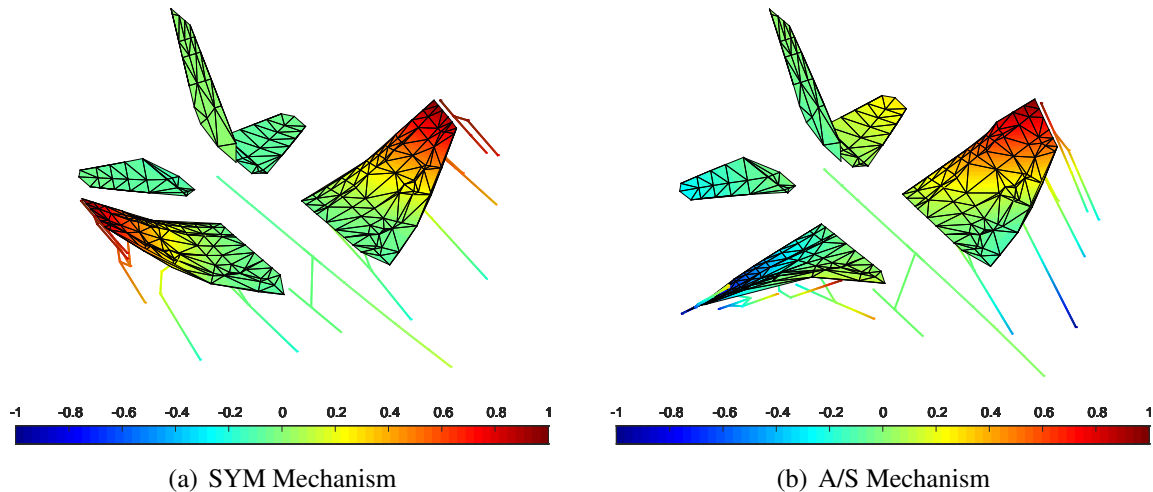


Figure 8: Flutter modes of the test configuration SYM and A/S mechanisms, colors by normalized deflection, Mach 0.95

4 RESULTS

The following sections 4.1-4.4 include investigations of store aerodynamics effects on the steady and unsteady surface pressure distributions, GAF matrices, and flutter solutions, respectively, based on the test configuration presented above. For these parts of the study, the AFC superposition methodology is not applied and direct GAF derivations are considered. Once underwing store effects are identified, section 4.5 presents validation study for the suggested AFC-superposition methodology for both ZAERO and ZEUS models. Several aerodynamic models are used for the purposes of these investigations: a basic model in which only the wingtip launchers are included, a model including both wingtip launchers and underwing missile stations, a model including the outboard wing span stations and midspan air-to-ground store stations, and a full aerodynamic model including all store stations. These four models are termed "1/9 stations", "1/9+2/8 stations", "1/9+2/8+3/7 stations" and "all stations", respectively.

4.1 Store Aerodynamics Effect on Steady Pressure Distributions

Figure 9 presents steady surface pressure distributions for the test configuration at Mach 0.95 conditions. For the ZAERO model, the presented distribution represent the normalized steady aerodynamic response to a variation in the aircraft angle of attack about zero angle of attack mean conditions. Since ZAERO assumes flat lifting surfaces, this surface pressure distribution represent the pressure differential ΔC_p between the upper and lower lift surfaces. For the ZEUS model, the presented distribution represents the nonlinear steady surface pressure coefficient C_p about 3° mean angle of attack conditions. From the ZEUS model results, it may be observed that at these high Mach conditions, the sonic zone along the upper wing surface stretches all the way near the trailing edge, where a strong shock wave is generated. This key flow phenomenon at these flow conditions is not captured by the linear ZAERO solution.

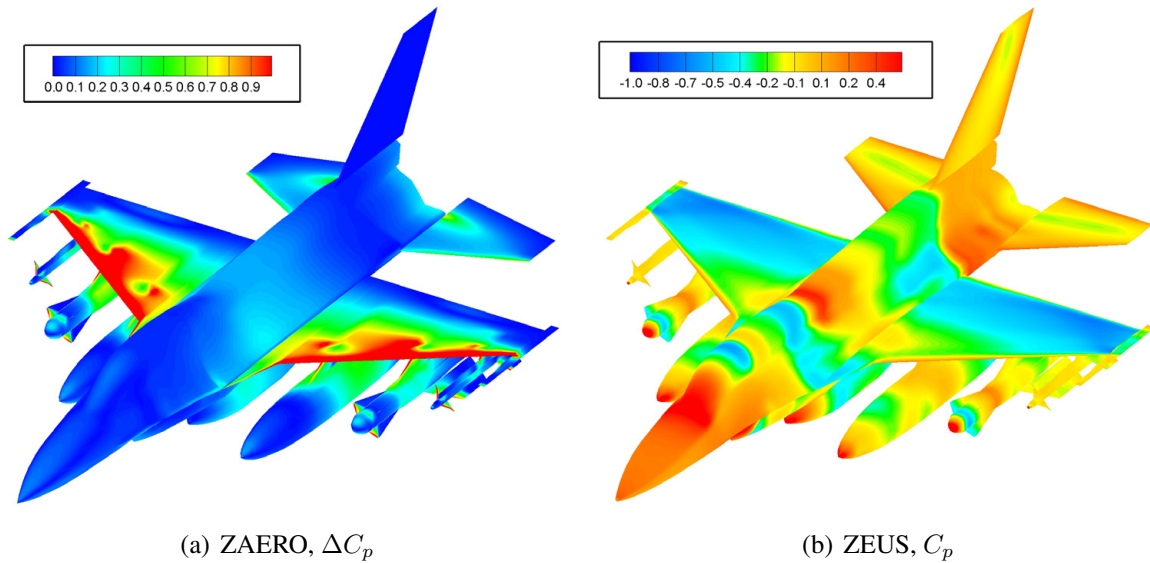


Figure 9: Steady flow surface pressure distributions, Mach 0.95

Figures 10- 13 present steady surface pressure distributions for the various underwing stores aerodynamic models in top and bottom wing views and for the ZAERO and ZEUS models. Focusing on the ZAERO ΔC_p distributions, underwing stores aerodynamics seem to affect the wing surface pressure differential distributions quite significantly (see Figures 10 and 11). Interestingly, the wing pressure variations due to store stations 2/8 and 3/7, as well as the pressure distributions along the stores surfaces themselves, remain similar for the full model. This suggests that for ZAERO linear models, interference effects between underwing store stations are minor. This indication supports the applicability of linear modeling approaches such as the one suggested in the current study. Focusing on the ZEUS C_p distributions, the upper surface does not seem to be affected much by any of the underwing store models (see Figure 12). On the other hand, the lower wing pressure distributions are more suspected to store aerodynamics effects, as observed in Figure 13. While the 2/8 store station effect is rather small, flow acceleration on the station 3/7 store decrease the pressure along the lower wing surface span (see Figure 13c). This effect is further magnified, as the station 4/6 fuel tank significantly affects the lower surface pressure distribution (see Figure 13d). A shock wave may be observed at the rear of fuel tank body, near the wing trailing edge. This shock expands along the wing lower surface span, thus affecting both the wing pressure distribution and the outer span stores surface pressures. Such flow phenomena are nonlinear in nature, therefore linear ROM modeling techniques are expected to offer poor prediction of such effects. Clearly the discussed steady flow observations may not directly indicate the significance of underwing stores aerodynamics for flutter prediction, however the apparent effects suggest that significant impact on unsteady aerodynamics characteristics may be expected.

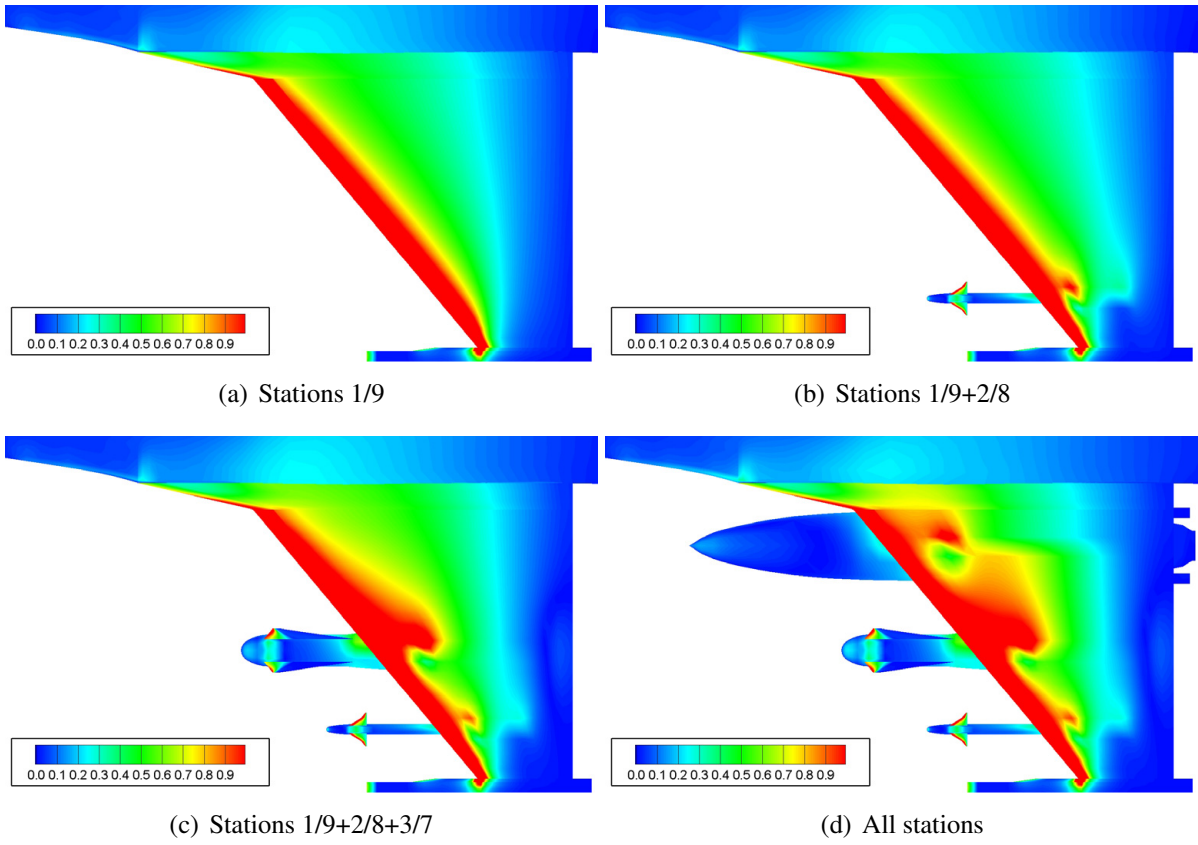


Figure 10: Steady flow surface ΔC_p distributions, top wing view, ZAERO model, Mach 0.95

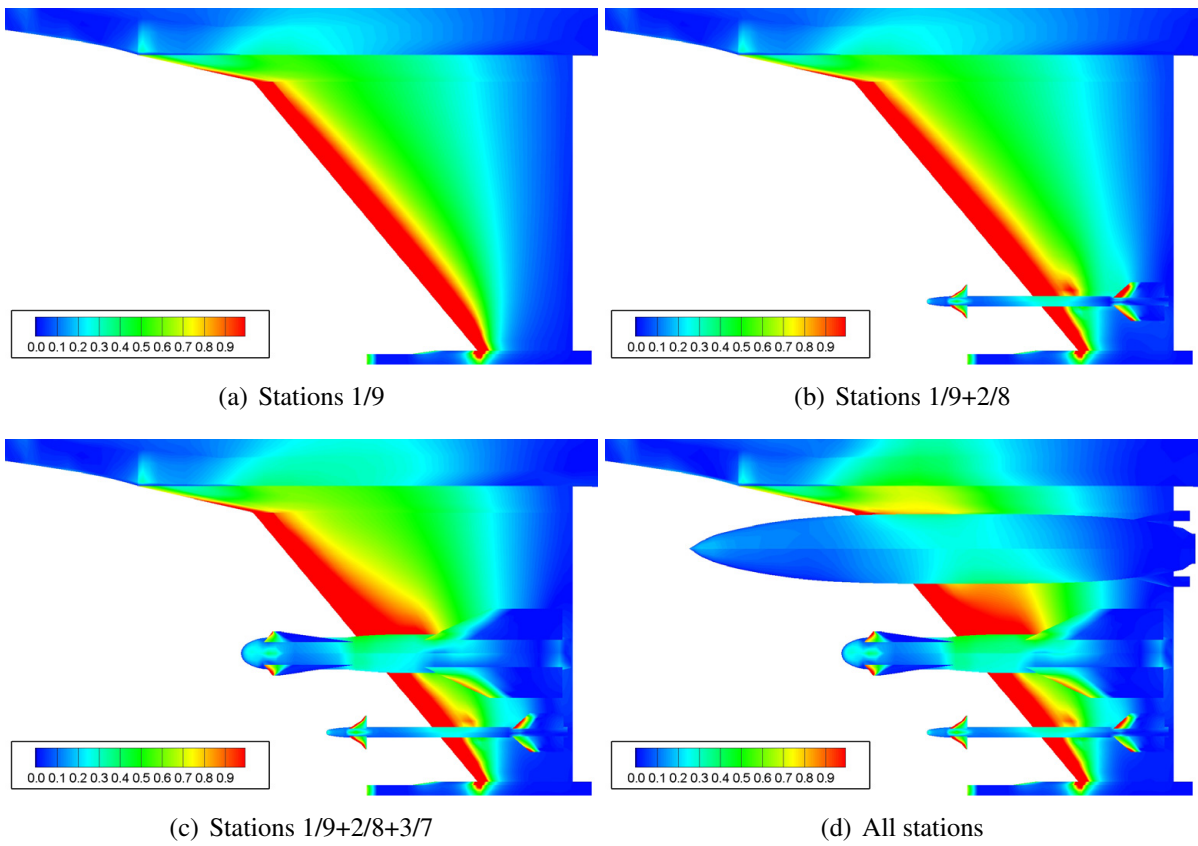


Figure 11: Steady flow surface ΔC_p distributions, bottom wing view, ZAERO model, Mach 0.95

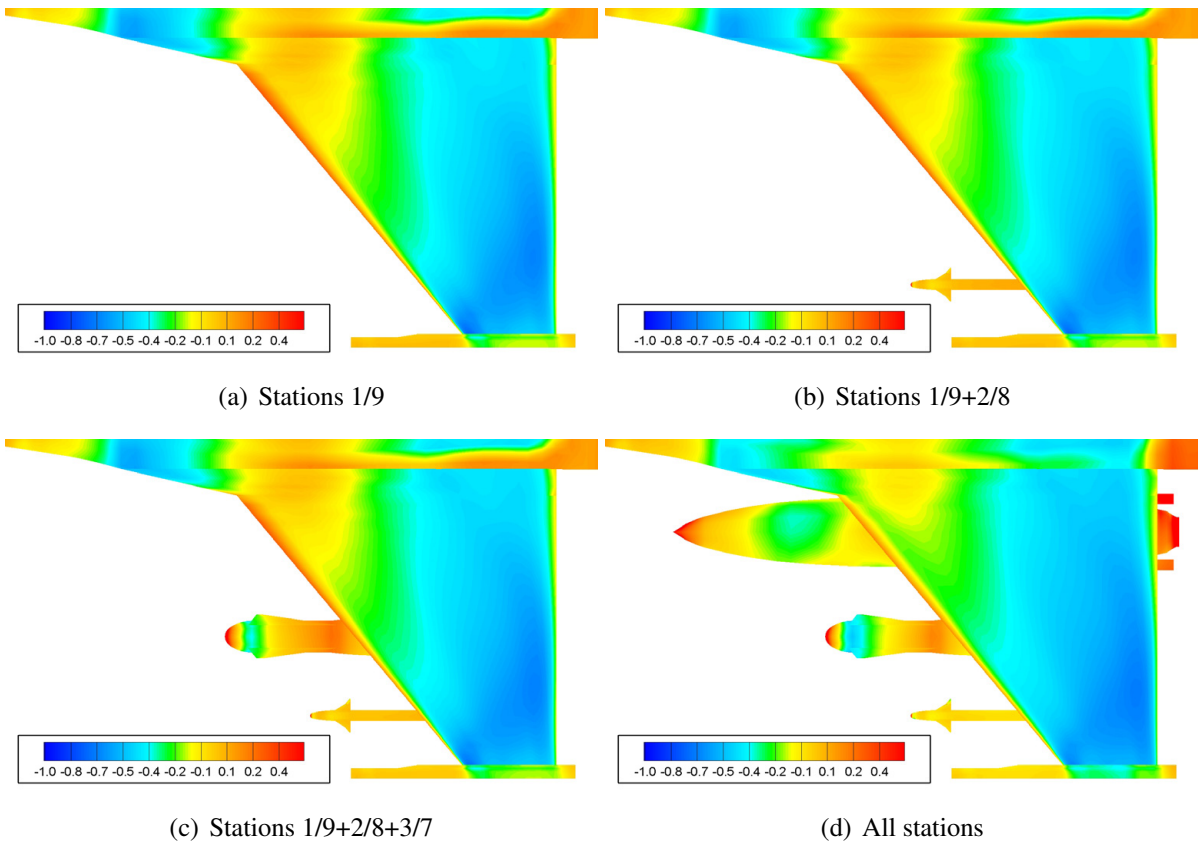


Figure 12: Steady flow surface C_p distributions, top wing view, ZEUS model, Mach 0.95, $\alpha = 3^\circ$

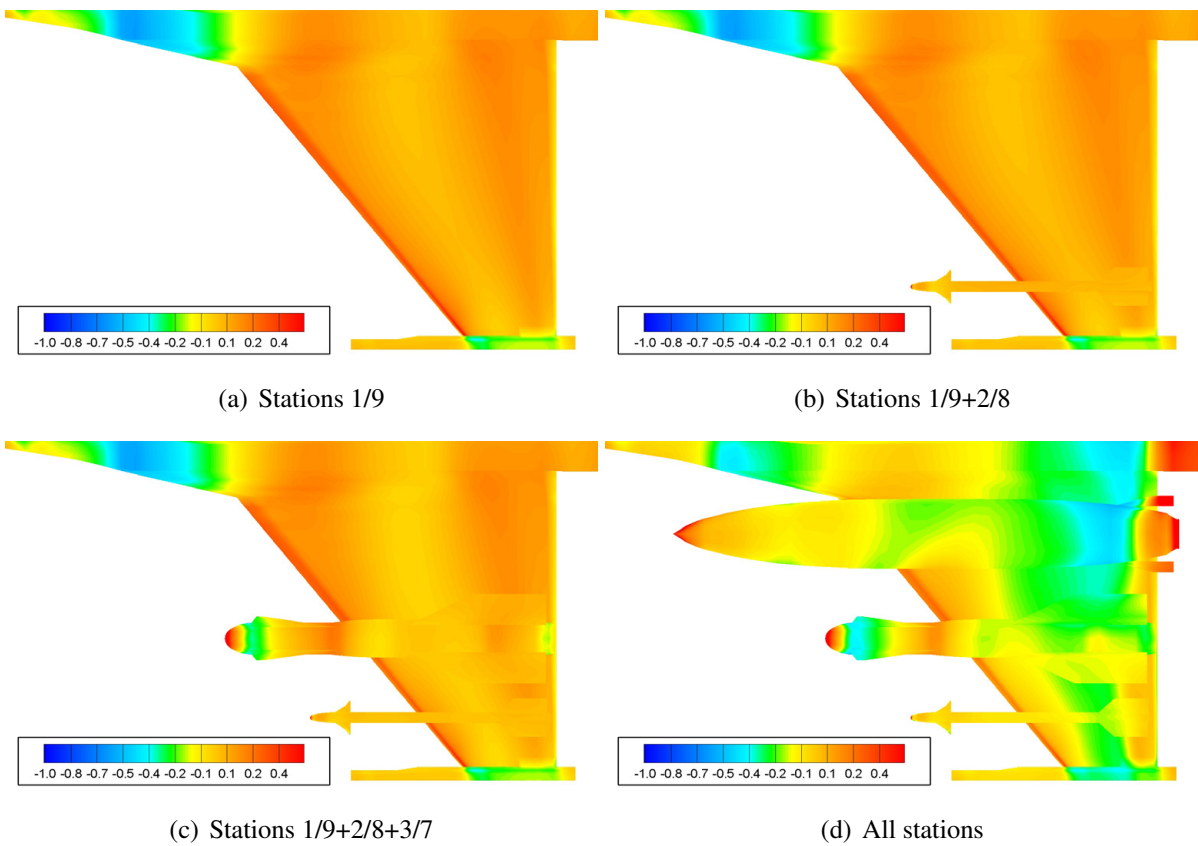


Figure 13: Steady flow surface C_p distributions, bottom wing view, ZEUS model, Mach 0.95, $\alpha = 3^\circ$

4.2 Store Aerodynamics Effect on Unsteady Pressure Distributions

Figure 14 presents unsteady surface pressure coefficient distributions $\Re\{ \Delta C'_p \}$ of the aerodynamic response to structural excitation in modes 3 (A/S) and 4 (SYM) at $k=0.2$ reduced frequency, which is approximately the flutter onset reduced frequency of the studied mechanisms. To allow comparison between the ZAERO and ZEUS models results, the ZEUS model results are presented on flat lifting surfaces as unsteady pressure differentials between the upper and lower surfaces, as in the ZAERO model. This comparison indicates that while at the forward wing region, unsteady pressure distributions between the models are generally similar, significant differences are identified near the wing trailing edge for both mode shape responses. These differences may be naturally attributed to the trailing edge shock and are consequently suspected to result in significant differences in flutter predictions between the ZAERO and ZEUS models.

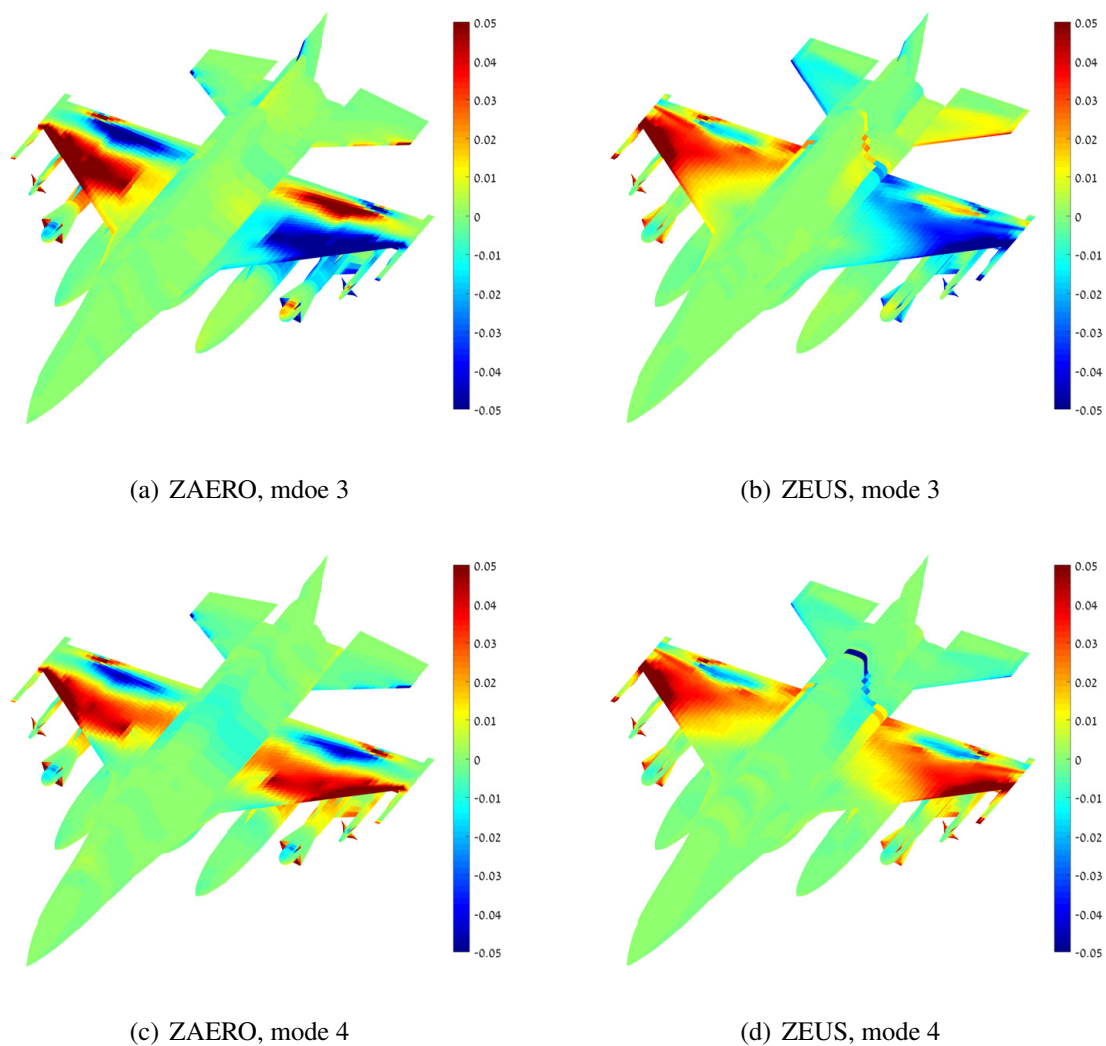


Figure 14: Unsteady flow pressure difference distributions $\Re\{ \Delta C'_p \}$ for modes 3 and 4, $k=0.2$, Mach 0.95

4.3 Store Aerodynamics Effect on GAF Matrices

In this section, store aerodynamics effects are assessed through study of the GAF matrix elements that correspond to the flutter coupling modes in each mechanism, as these elements most significantly affect each flutter solution. Figures 15- 18 present variations of real and imaginary GAF elements parts with reduced frequency k for the various aerodynamic models for the SYM and A/S mechanism coupling modes. The dotted red lines indicates the reduced frequency at flutter conditions, which is approximately $k = 0.2$ for both mechanisms. For all cases, aerodynamic damping (imaginary parts) magnitudes increase with k as more store stations are included in the aerodynamic model, which allegedly should alleviate flutter onset conditions. Nevertheless, at flutter reduced frequency conditions, this increase in aerodynamic damping is shown to be insignificant. On the other hand, aerodynamic stiffness (real parts) is much more considerably affected by stores modeling in both ZAERO and ZEUS models, as the stiffness curves are biased across the entire reduced frequency band. For the SYM mechanism ZAERO model GAFs (Figure 15), stores modeling increase the stiffness curves for the mode 5 related GAFs by up to 100% at flutter reduced frequency conditions, while the mode 4 related GAFs stiffness curves are almost unaffected at these conditions. For the SYM mechanism ZEUS model GAFs (Figure 16), the mode 4 related stiffness curves vary by up to 100% due to stores modeling, while the mode 5 related GAFs are hardly affected. These trends decrease the aeroelastic frequency of mode 5 in the ZAERO model and increase the aeroelastic frequency of mode 4 in the ZEUS model, and thereby reinforces the modes coupling and reduces the flutter onset speed for this mechanism in both models, as demonstrated in section 4.4. For the A/S mechanism GAFs (Figures 17- 18), significant stiffness curves variations of up to 100% are identified due to stores modeling in both modes 3 and 6 of the ZAERO and ZEUS models. Similarly to the SYM mechanism, this decrease in the mode 3 related stiffness curves and increase in the mode 6 stiffness are expected to influence the aeroelastic frequencies such that mode 3 frequency is increased and mode 6 frequency is decreased, hence the modes coupling is reinforced and flutter onsets are expected at lower speeds. Although the overall agreement in trends between the ZAERO and ZEUS models GAF variations, the absolute GAF curves compare poorly between the models. This is once again attributed to the significant differences in flow solutions at the examination high transonic flow conditions.

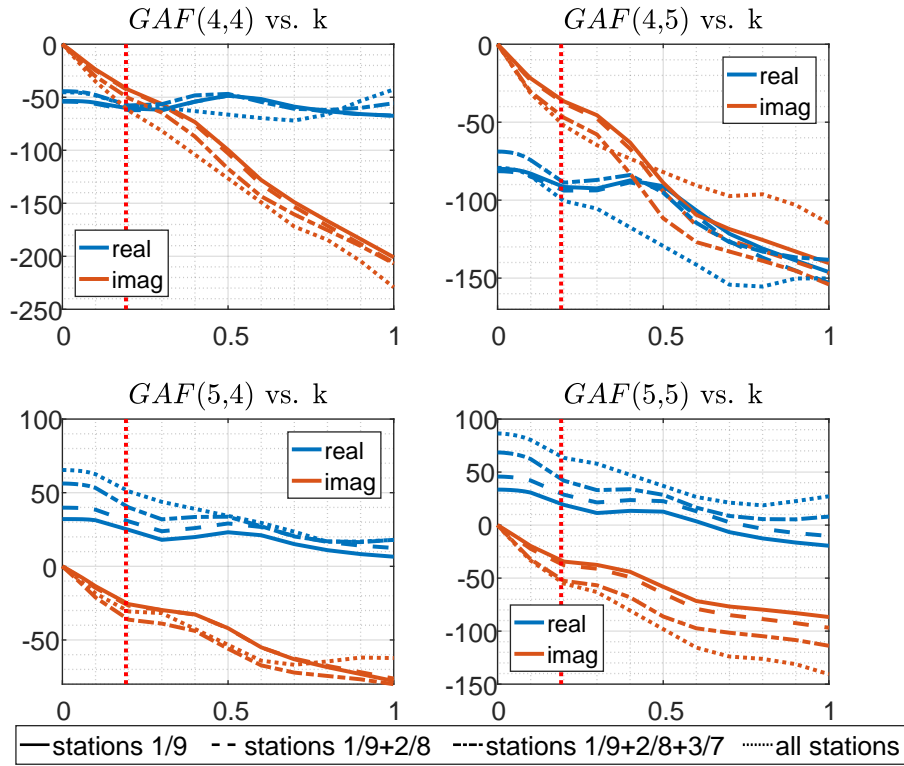


Figure 15: GAFs variation with normalized reduced frequency using various ZAERO aerodynamic models, flutter coupling modes of the SYM mechanism, Mach 0.95, red dotted line indicates flutter mechanism conditions

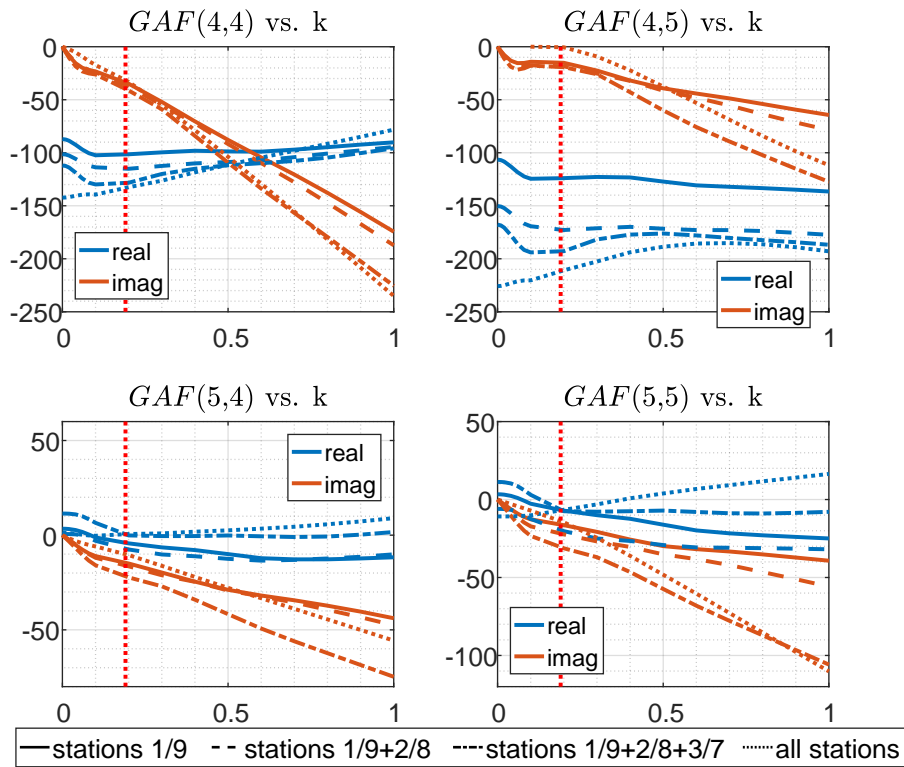


Figure 16: GAFs variation with normalized reduced frequency using various ZEUS aerodynamic models, flutter coupling modes of the SYM mechanism, Mach 0.95, red dotted line indicates flutter mechanism conditions

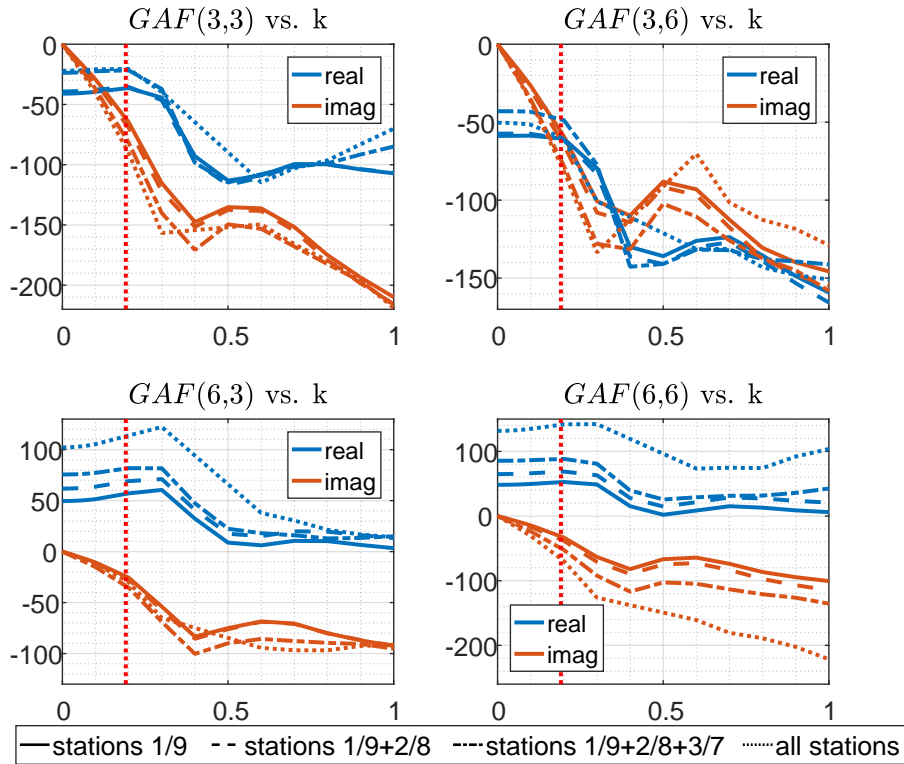


Figure 17: GAFs variation with normalized reduced frequency using various ZAERO aerodynamic models, flutter coupling modes of the A/S mechanism, Mach 0.95, red dotted line indicates flutter mechanism conditions

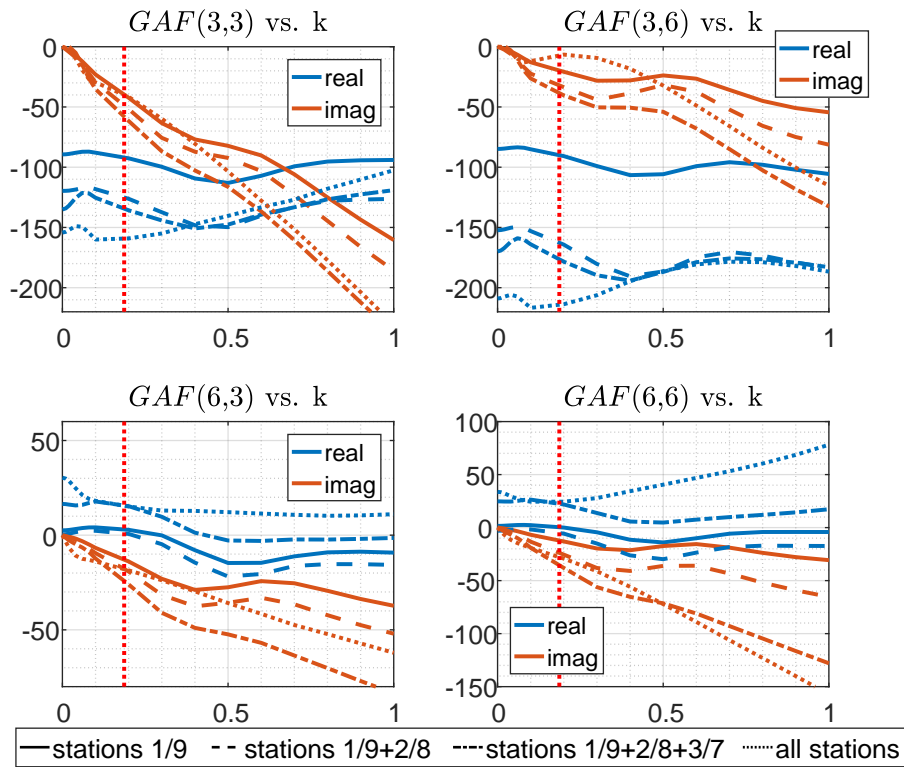


Figure 18: GAFs variation with normalized reduced frequency using various ZEUS aerodynamic models, flutter coupling modes of the A/S mechanism, Mach 0.95, red dotted line indicates flutter mechanism conditions

4.4 Store Aerodynamics Effect on the Flutter Solution

Store aerodynamics effects on the flutter solution are presented in Figure 19 for the ZAERO and ZEUS models. As predicted by the previous investigations, both mechanisms are strongly affected by the inclusion of underwing stores into the aerodynamic model in both ZAERO and ZEUS. For both models, the GAF stiffness trends which were identified in the previous section are well observed in the frequency curves presented in Figures 19a and 19c, as the frequency separation of the coupling modes is decreasing for both mechanisms as more underwing stores are included. In the ZAERO model solution, both the SYM and A/S mechanism flutter speeds are decreased by about 15% EAS for the full aerodynamic model compared with the basic tip launchers model (see Figure 19b). The full aerodynamic model results are in better agreement with the A/S LCO onset FT boundary, which is overpredicted by the ZAERO model by about 15% EAS. Still, according to this model, the SYM mechanism remains the more dominant hard flutter case and its predicted onset speed is within the FT cleared envelope. In the ZEUS model solution, both mechanisms flutter speeds are decreasing as more underwing stores are included in the aerodynamic model (see Figure 19d). While the SYM mechanism remains a hump mechanism, the A/S mechanism becomes a hard flutter case as its onset speed prediction is decreased by about 30% EAS for the full aerodynamic model compared with the basic tip launchers model. This prediction is in excellent agreement of 5% EAS with the A/S LCO onset FT indication. These results suggest that underwing stores aerodynamic modeling may offer both a more realistic and conservative prediction capability.

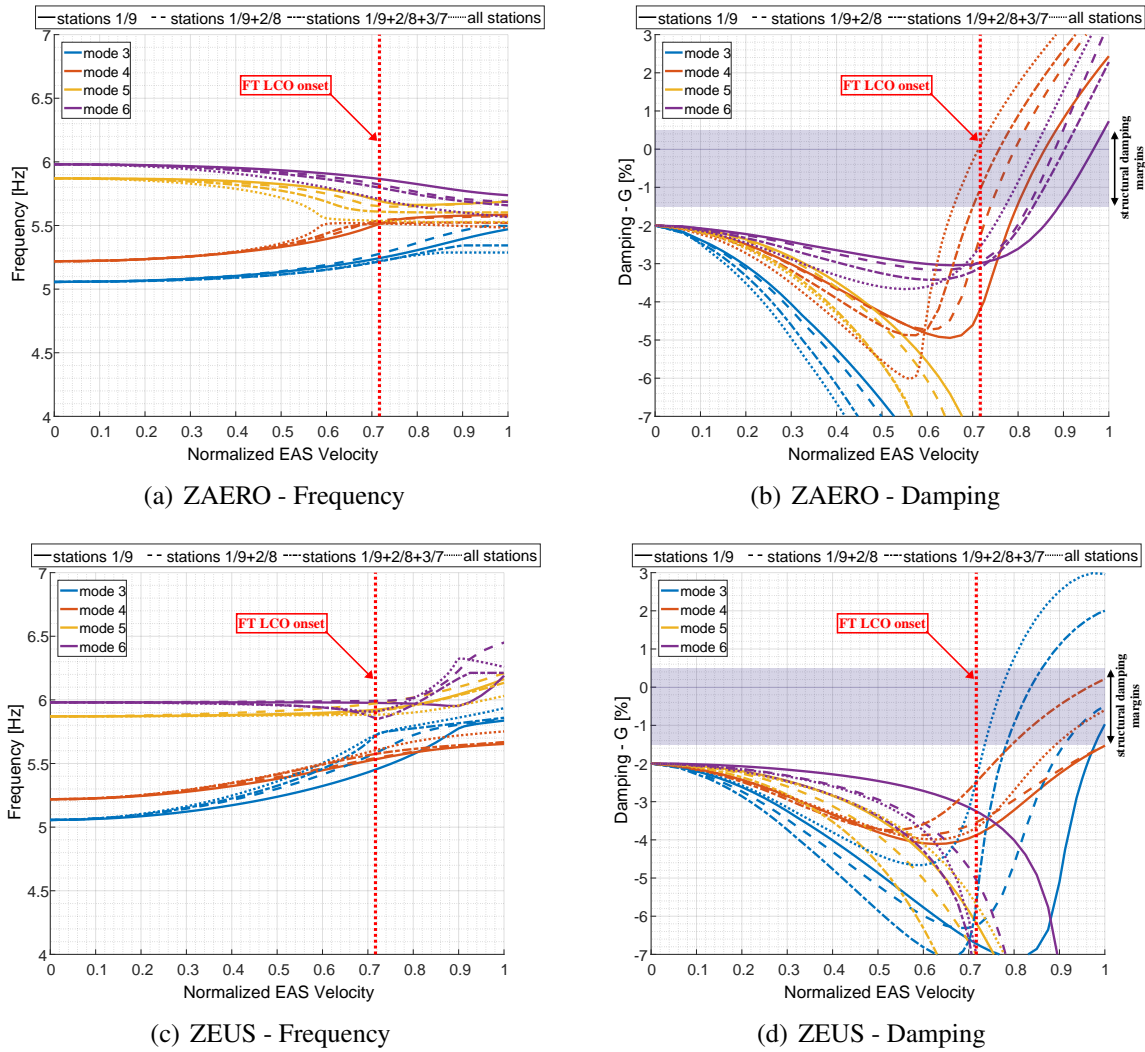


Figure 19: Flutter analyses results using various aerodynamic models, Mach 0.95

4.5 Validation of Stores Aerodynamic Model Superposition Method

The AFC superposition method that was presented in the Theoretical Model section is validated in this section by means of comparison between flutter analyses results obtained using direct calculation of the AFC matrix and assembly of the AFC based on pre-calculated component AFC_i submatrices according to the suggested method procedure. This comparison is presented in Figures 20- 23 for aerodynamic models including the various span stations incrementally. For the ZAERO models solutions, good correlation between frequency and damping curves is obtained around flutter conditions, although some differences between the solutions may be observed at high modal damping conditions. Since flutter analysis results are mainly meaningful at low damping conditions, these comparisons support the effectiveness of the suggested superposition approach for panel based solvers in obtaining reliable flutter predictions including store aerodynamics effects. For the ZEUS models, fairly good agreement between the direct and superposition solutions is obtained for the stations 1/9 (see Figure 20d) and stations 1/9+2/8 (see Figure 21d) models. As more inboard store stations are included in the model, its effects are only partially captured by the superposition solution, as indicated in Figures 22d and 23d. This suggests that the inboard stores interference with the wing, as well as with the other stores, is nonlinear, and hence can not be captured accurately by linear superposition techniques. This indication is also supported by the steady surface pressure investigation observations presented

in section 4.1. It may be argued that such modeling approach of nonlinear CFD-ROM models, despite its limitation to account for nonlinear interference effects such are presented above, is still preferable over any linear panel-based model, since when using this approach the base flow nonlinear effects are better captured.

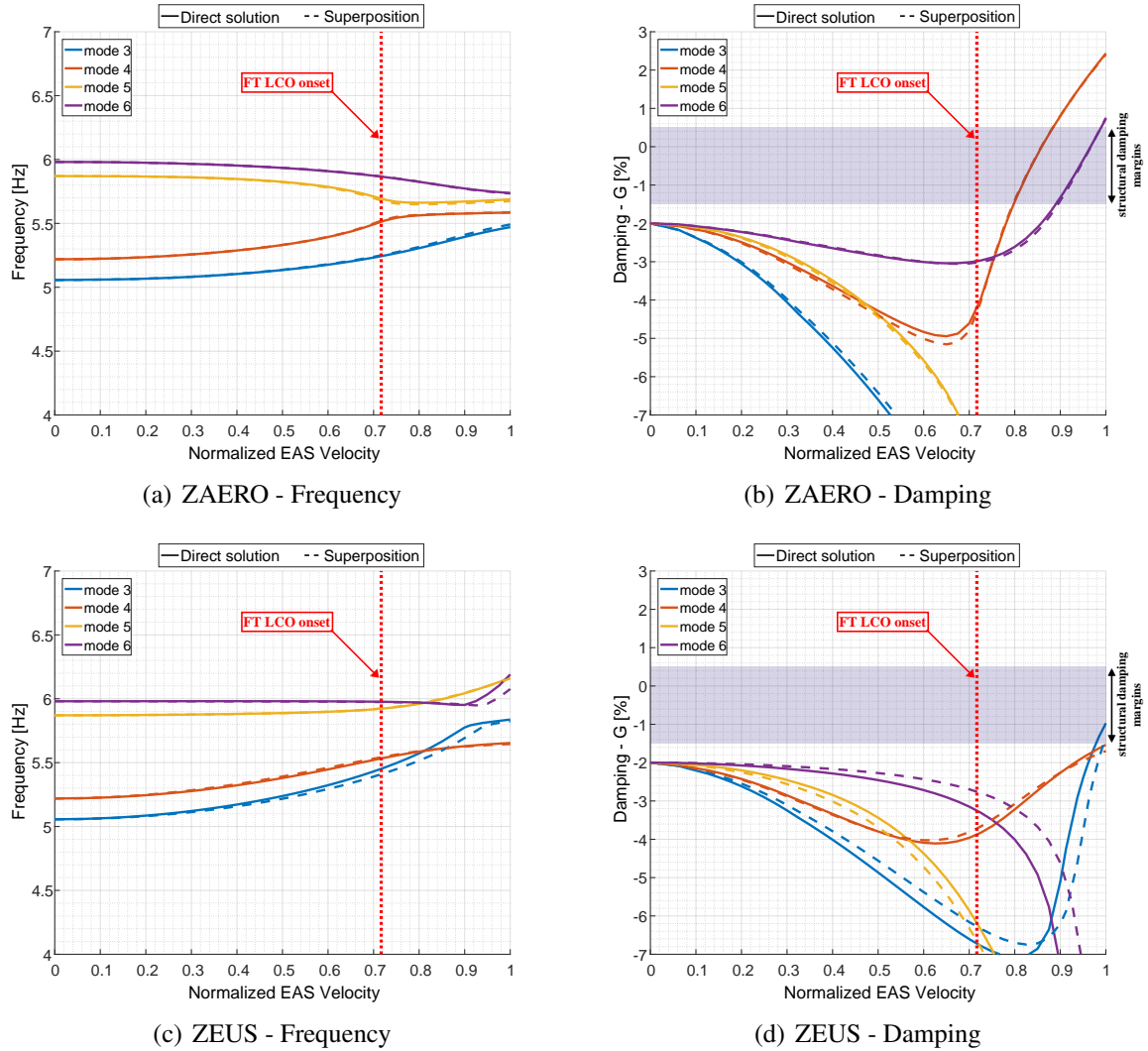
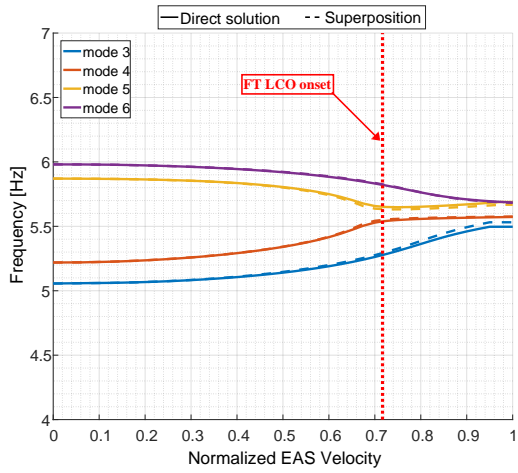
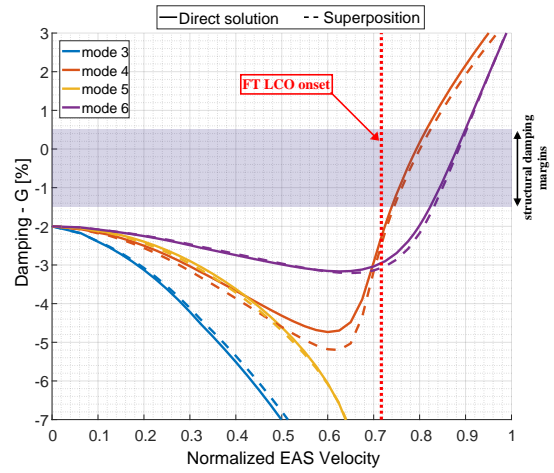


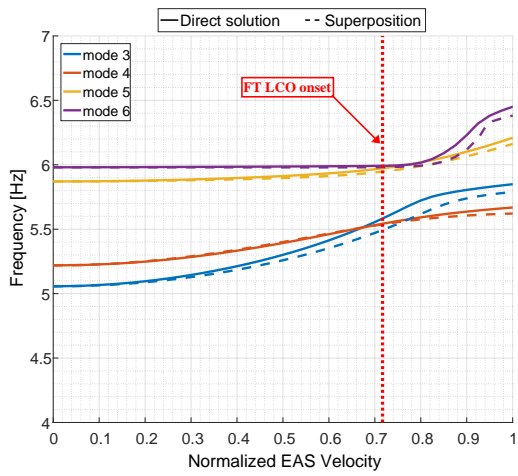
Figure 20: Flutter analyses results using stations 1/9 aerodynamic models, Mach 0.95



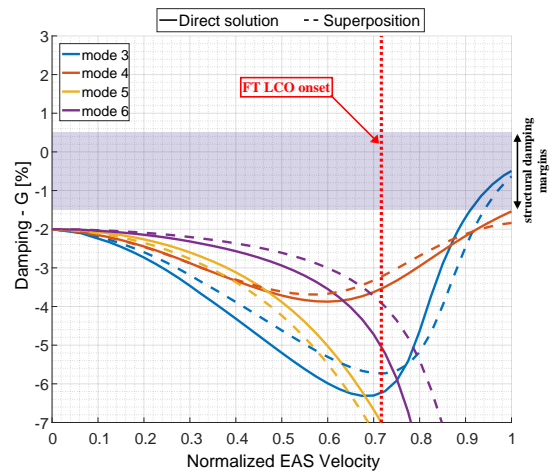
(a) ZAERO - Frequency



(b) ZAERO - Damping

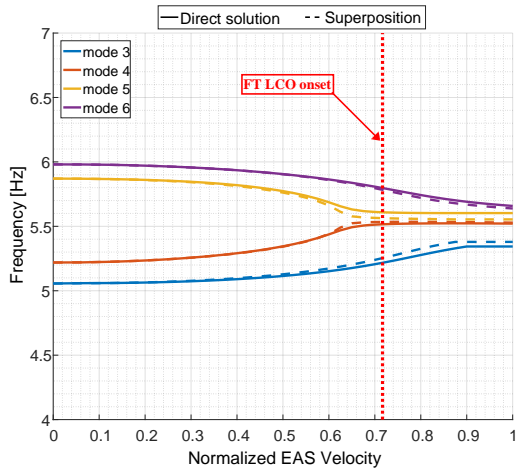


(c) ZEUS - Frequency

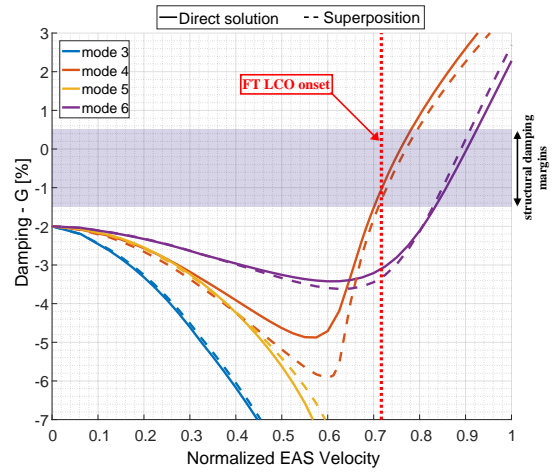


(d) ZEUS - Damping

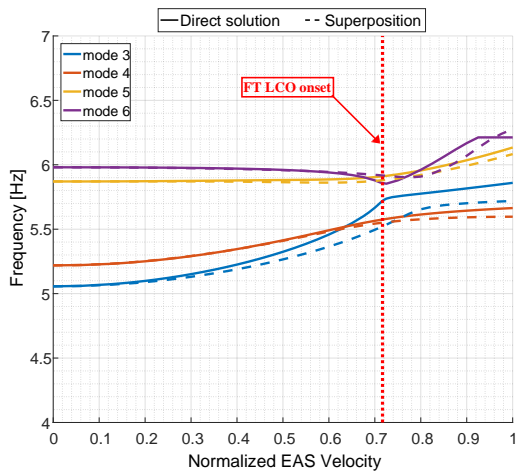
Figure 21: Flutter analyses results using stations 1/9+2/8 aerodynamic models, Mach 0.95



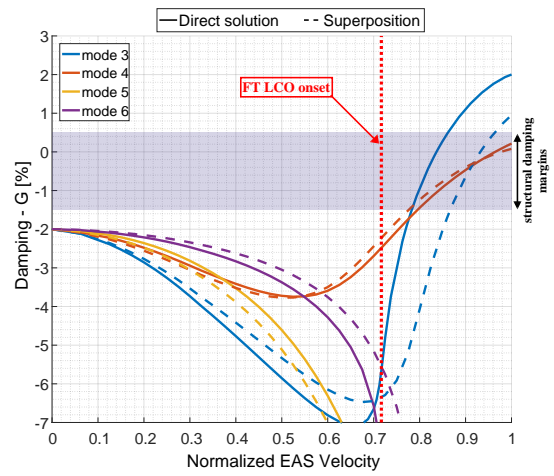
(a) ZAERO - Frequency



(b) ZAERO - Damping

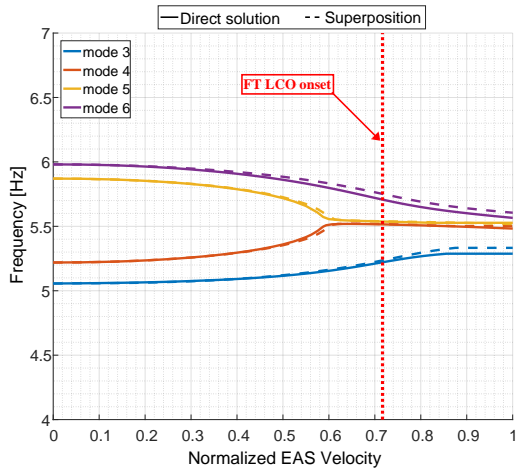


(c) ZEUS - Frequency

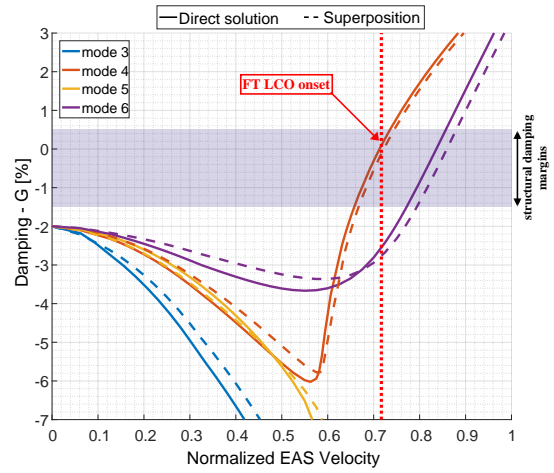


(d) ZEUS - Damping

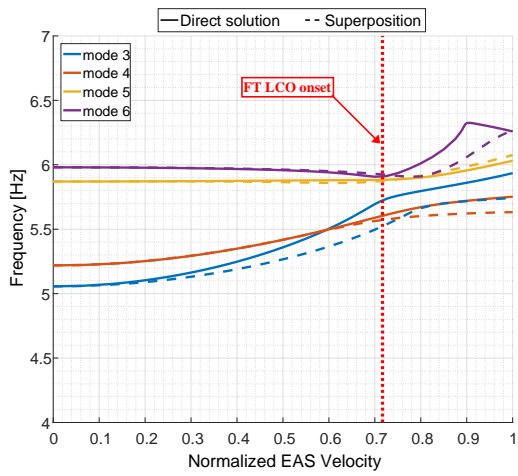
Figure 22: Flutter analyses results using stations 1/9+2/8+3/7 aerodynamic models, Mach 0.95



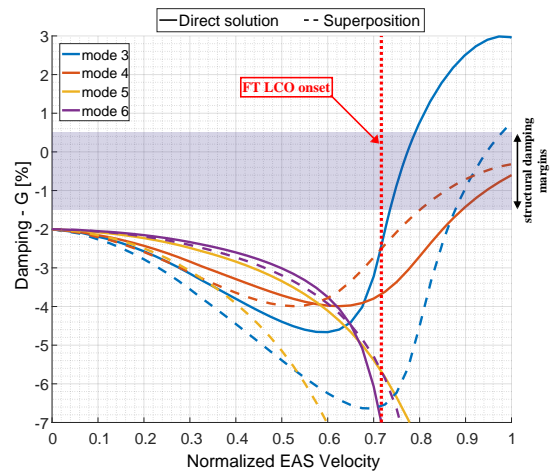
(a) ZAERO - Frequency



(b) ZAERO - Damping



(c) ZEUS - Frequency



(d) ZEUS - Damping

Figure 23: Flutter analyses results using all stations aerodynamic models, Mach 0.95

5 SUMMARY AND DISCUSSION

The current study deals with two issues related to fighter aircrafts underwing stores unsteady aerodynamics. The first issue is assessment of the effects of underwing stores aerodynamics on analytic flutter predictions. The second issue is evaluation of a superposition modeling approach which may enable inclusion of underwing stores effects without drastically affecting the computational costs of industrial fighter aircrafts flutter analysis surveys. For both purposes, a heavyweight store configuration of the F-16 aircraft with underwing stores was studied at high transonic flow conditions and flutter predictions were correlated with flight test indications of LCO onset conditions. The investigation was conducted using two unsteady aerodynamics solvers, namely, the linear, panel-based, ZAERO solver, which is the industrial standard for flutter predictions, and the nonlinear, Cartesian grids-based, ZEUS Euler solver.

The assessment of underwing store aerodynamics effects showed that underwing stores modeling may in-fact considerably affect flutter predictions. The studied test configuration SYM and A/S flutter mechanisms were mainly affected by underwing stores modeling through aerodynamic stiffness variations which resulted in up to 15% and 30% decrease in predicted flutter onset speeds for the ZAERO and ZEUS models, respectively. For a typical fighter aircraft, such variation in flutter speed may be translated to more than 150 knots. For this case, neglecting stores aerodynamics yielded both less realistic and nonconservative predictions.

At the examination high transonic Mach conditions, significant differences between the ZAERO and ZEUS solutions were identified in terms of steady and unsteady surface pressure distributions, GAF matrices variations, and flutter analysis frequency-damping curves trends. These differences are generally attributed to the strong shock waves that appear on the wing and stores surfaces, which are not captured by the ZAERO solver. These differences manifested in a key missprediction of the SYM mechanism nature and onset speeds by the ZAERO model. While the ZAERO model analysis identifies this mechanism as a hard flutter case with onset speed within the FT cleared envelope, the same mechanism is identified as a hump mode by the ZEUS model analysis. Considering full aerodynamic models with all underwing stores included, the ZAERO model analysis yielded fair agreement with the A/S mechanism FT LCO onset reference with a 15% EAS over-prediction, while the ZEUS model analysis yielded better correlation of a 5% overprediction compared with the reference boundary.

A novel store aerodynamics superposition modeling approach was formulated and validated. The suggested approach results were compared with results obtained using a direct modeling approach using both ZAERO and ZEUS models. For ZAERO models, this comparison showed sufficient agreement between the two approaches even when including all underwing store stations in the model. For ZEUS models, the outboard wing station stores effects were captured correctly by the method, while the inboard stores effects were not captured as correctly. This indication is in general agreement with the observations made by comparing between various ZEUS underwing stores models in terms of steady surface pressure distributions. In this investigation, the interaction between inboard and outboard span stores was found to be nonlinear due to shock waves which are generated on the inboard span stores surfaces. Consequently, the suggested modeling approach is shown to be applicable for linearized CFD-based ROM aerodynamic databases construction, as long as nonlinear interference effects between store stations are not dominant. The suggested approach may potentially enable direct integration of high-fidelity computational aeroelasticity modeling capabilities with industrial flutter analysis frameworks in a straightforward way, under the indicated limitations. The computational costs required by the suggested approach are limited to the aerodynamic database construction pro-

cess, thus it is applicable to industrial flutter analysis surveys of thousands of configurations in a reasonable computational cost.

6 REFERENCES

- [1] Guyan, R. (1965). Reduction of Stiffness and Mass Matrices. *AIAA Journal*, 3(2), 380–380. doi:10.2514/3.56887.
- [2] Duchon, J. (1976). *Constructive Theory of Functions of Several Variables. Lecture Notes in Mathematics*, vol. 571, chap. Splines Minimizing Rotation-Invariant Semi-Norms in Sobolev Spaces. Berlin, Heidelberg: Springer. doi:10.1007/BFb0086566.
- [3] Rodden, W. and Johnson, E. (1994). *MSC.NASTRAN Aeroelastic Analysis Users Guide Version 68*. The MacNeal-Schwendler Corporation Publication.
- [4] ZONA Technology, Scottsdale, AZ (2016). *ZAERO Theoretical Manual, Version 9.2*, 1 ed. ZONA 02-12.4.
- [5] Bendiksen, O. (2001). Transonic Flutter and the Nature of the Transonic Dip. In *International Forum on Aeroelasticity and Structural Dynamics*, vol. Vol. II. pp. 273–286.
- [6] Raveh, D. (2004). Identification of Computational-Fluid-Dynamics Based Unsteady Aerodynamic Models for Aeroelastic Analysis. *Journal of Aircraft*, 41(3), 620–632. doi: 10.2514/1.3149.
- [7] Cavagna, L., Quaranta, G., and Mantegazza, P. (2007). Application of NavierStokes simulations for aeroelastic stability assessment in transonic regime. *Computers and Structures*, 85, 818–832. doi:10.1016/j.compstruc.2007.01.005.
- [8] Heeg, J., Wieseman, C., and Chwalowski, P. (2016). Data Comparisons and Summary of the Second Aeroelastic Prediction Workshop. In *AIAA 34th Applied Aerodynamics Conference*. Reston, VA: AIAA. doi:10.2514/6.2016-3121. AIAA-2016-3121.
- [9] Turner, C. (1981). Effect of Store Aerodynamics on Wing/Store Flutter. *Journal of Aircraft*, 19(7), 574–580. doi:10.2514/3.57431. AIAA-81-0604R.
- [10] Albano, E. and Rodden, W. (1969). A Doublet-Lattice Method for Calculating Lift Distributions on Oscillating Surfaces in Subsonic Flows. *AIAA Journal*, 7(2), 279–285. doi: 10.2514/6.1968-73.
- [11] Chen, P., Sulaeman, E., Liu, D., et al. (2002). Influence of External Store Aerodynamics on Flutter/LCO of a Fighter Aircraft. In *AIAA 43rd Structures, Structural Dynamics and Materials Conference*. Reston, VA: AIAA. doi:10.2514/6.2002-1410. AIAA-2002-1410.
- [12] Maxwell, D., Denegri, C., Dawson, K., et al. (2007). Effect of Underwing Store Aerodynamics on Analytically Predicted F-16 Aeroelastic Instability. In *AIAA 48th Structures, Structural Dynamics and Materials Conference*. Reston, VA: AIAA. doi: 10.2514/6.2007-2366. AIAA-2007-2366.
- [13] Lee, D. and Chen, P. (2002). Studies of Aerodynamic Influence of Under-Wing Stores on Flutter Characteristics of F-16. In *AIAA 50th Structures, Structural Dynamics and Materials Conference*. Reston, VA: AIAA. doi:10.2514/6.2009-2463. AIAA-2009-2463.

- [14] Chen, P. (1993). Unsteady Subsonic Aerodynamics for Bodies and Wings with External Stores Including Wake Effect. *Journal of Aircraft*, 30(5), 618–628. doi:10.2514/3.46390.
- [15] Terashima, H. and Fujii, K. (2007). Influence of the Store on the Transonic and Supersonic Flutter Characteristics of a Delta Wing Configuration. *Journal of Aircraft*, 45(1), 237–246. doi:10.2514/3.46390.
- [16] Karpel, M., Moulin, B., Anguita, L., et al. (2004). Flutter Analysis of Aircraft with External Stores Using Modal Coupling. *Journal of Aircraft*, 41(4), 892–902. doi:10.2514/1.11483.
- [17] Karpel, M. and Raveh, D. (1995). The Fictitious Mass Element in Structural Dynamics. In *AIAA 36th Structures, Structural Dynamics and Materials Conference*. Reston, VA: AIAA. doi:10.2514/6.1995-1343. AIAA-95-1343-CP.
- [18] ZONA Technology, Scottsdale, AZ (2015). *ZEUS Users Manual, Version 3.9*, 2 ed. ZONA 09-18.
- [19] Zhang, Z., Yang, S., and Chen, P. (2009). Linearized Euler Solver for Rapid Frequency-Domain Aeroelastic Analysis. *Journal Of Aircraft*, 49(3), 922–932. doi:10.2514/1.C031611.
- [20] Gu, Y. and Yang, Z. (2012). Modified p-k Method for Flutter Solution with Damping Iteration. *AIAA Journal*, 50(2), 507–510. doi:10.2514/1.J051360.

COPYRIGHT STATEMENT

The authors confirm that they, and/or their company or organization, hold copyright on all of the original material included in this paper. The authors also confirm that they have obtained permission, from the copyright holder of any third party material included in this paper, to publish it as part of their paper. The authors confirm that they give permission, or have obtained permission from the copyright holder of this paper, for the publication and distribution of this paper as part of the IFASD-2019 proceedings or as individual off-prints from the proceedings.